

Numerical detection of symmetry enriched topological phases with space group symmetry

Ling Wang,^{1,2} Andrew Essin,^{1,2} Michael Hermele,³ and Olexei Motrunich²

¹*Institute for Quantum Information and Matter,*

California Institute of Technology, Pasadena, California 91125, USA

²*Department of Physics, California Institute of Technology, Pasadena, California 91125, USA*

³*Department of Physics, 390 UCB, University of Colorado, Boulder CO 80309, USA*

(Dated: July 28, 2021)

Topologically ordered phases of matter, in particular so-called symmetry enriched topological (SET) phases, can exhibit quantum number fractionalization in the presence of global symmetry. In \mathbb{Z}_2 topologically ordered states in two dimensions, fundamental translations T_x and T_y acting on anyons can either commute or anticommute. This property, crystal momentum fractionalization, can be seen in a periodicity of the excited-state spectrum in the Brillouin zone. We present a numerical method to detect the presence of this form of symmetry enrichment given a projected entangled pair state (PEPS); we study the minima of spectrum of correlation lengths of the transfer matrix for a cylinder. As a benchmark, we demonstrate our method using a modified toric code model with perturbation. An enhanced periodicity in momentum clearly reveals the nontrivial anticommutation relation $\{T_x, T_y\} = 0$ for the corresponding quasiparticles in the system.

PACS numbers: 05.30.Pr, 71.15.Qe, 75.10.Jm, 75.10.Kt

Topological order is the name given to a variety of long range entangled but gapped phases of matter, in particular to phases that support anyonic excitations with unusual braiding statistics. Unlike phases that fall within the Landau symmetry-breaking paradigm, topological order is defined without any reference to symmetry. However, it is still very interesting to ask what further phenomena emerge in systems with symmetry, either spontaneously broken or unbroken. The term “symmetry enriched topological” (SET) phases was proposed to describe phases that have the same topological order but are distinct in the presence of a symmetry [1–3].

In two dimensions the excitations in a topological phase are point-like anyons. When a symmetry is present, what are their quantum numbers? It turns out that these can be fractional; most prominently, anyons in quantum Hall states typically have fractional electric charge (the quantum number corresponding to a $U(1)$ symmetry of the system) [4, 5]. The values of these quantum numbers are highly constrained, notably by the “fusion rules” of the topological theory; in the Laughlin quantum Hall state with filling fraction $1/3$, since three anyons give back an electron, the anyons must have charge $e/3$. Another example is the spin fractionalization in spin liquid phases of quantum magnets with a global $SU(2)$ symmetry: a spinon quasiparticle carries a fractional number spin- $1/2$ whereas in conventional paramagnets or magnetically ordered states all quasiparticles carry integer spin [6].

Can one distinguish SET phases given a wavefunction? The quantum numbers of the degenerate ground states and the projective quantum numbers of quasiparticles are the characteristic properties of the SET phases [2, 7–9]. In the case of detecting the projective quantum number

of an internal symmetry, the operation of the global internal symmetry generator can be factorized into a product of local operators, which can be transformed into operators acting only on the entanglement cut of the system, therefore one can detect the projective quantum number via measuring the commutator/anti-commutator of the boundary quasiparticles [10, 11]. However for the space group symmetry, such as the translation symmetries, the translation operator is written in a matrix product operator that can not be factorized, and in addition, there is no way to make an entanglement cut that preserves both T_x and T_y translations, therefore conventional techniques do not work. In this Letter, we address this question for space group symmetries in the context of projected entangled pair states (PEPSs) [12].

\mathbb{Z}_2 topological phases with translation symmetry – We are interested in the topological order familiar from \mathbb{Z}_2 gauge theory, \mathbb{Z}_2 spin liquids, and the toric code. There are two bosonic anyon species, often called e and m . Each sees the other with an Aharonov-Bohm phase of -1 (they are mutual semions). When two-dimensional translation symmetry is present, the symmetry generators T_x and T_y may act nontrivially (projectively) on the anyons [2, 13]. A basis-independent characterization of these actions is given by the relations

$$\begin{aligned} T_x^e T_y^e T_x^{e-1} T_y^{e-1} &= \eta_e = \pm 1, \\ T_x^m T_y^m T_x^{m-1} T_y^{m-1} &= \eta_m = \pm 1, \end{aligned} \quad (1)$$

where T_x^e is the action of T_x on a single e , etc. When one of these relations evaluates to -1 we say that translations act projectively, or that the anyon has fractional crystal momentum or has nontrivial fractionalization class, a notion closely related to Wen’s projective symmetry group [14].

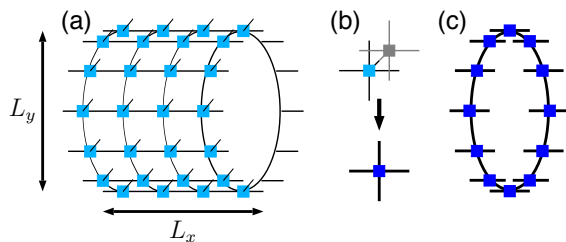


FIG. 1: (a) Schematic representation of a PEPS on a cylinder of size $L_x \times L_y$. (b) When multiplying bra and ket of PEPS, we sum over the physical degrees of freedom, group the virtual indices of a bond, and arrive at the double tensor of a single site. (c) Placing L_y double tensors on a ring and tracing out the virtual degrees on the shared bonds, we form the transfer matrix of the cylinder.

One can interpret the nontrivial e relation as the presence of an m in each unit cell of the lattice, which the e sees as a background π magnetic flux. It is straightforward to show, based on this observation or directly from the relations above, that if e has fractional crystal momentum, the spectrum (and density of states) of two- e scattering states is periodic under $\mathbf{q} \rightarrow \mathbf{q} + (\pi, 0), (0, \pi), (\pi, \pi)$ [13, 15]. Assuming that e is the excitation of lowest energy, the low-energy edge of the continuum of excited states will reveal the fractionalization class of e in the dynamical structure factor of any operator that excites anyons. This is the main idea for detecting such SET states that we pursue in this paper. However, we access the low-energy edge of the excited states via the information contained in the ground state instead of the excitation spectrum due to a nice property given by the PEPS, which we will introduce below.

PEPS and transfer matrix – PEPS is an ansatz that represents the wavefunction by locally entangled virtual pairs and a projector that map the virtual system to the physical one [16]. It captures a wide range of phases including many with topological order [17–24]. A one-dimensional version, the MPS [25], has been used to classify phases of symmetric, gapped spin systems based on the projective representation of the symmetry group [26–28]. Here, we propose a method based on PEPS for the spectra of correlation lengths (SCL) of the system, which allows us to distinguish SET phases described by simple PEPSs.

In one-dimensional gapped systems, properties of the ground state wave function (the MPS) are completely determined by the transfer matrix if translation symmetry is present. The spectrum of correlation lengths, which is given by the negative of the logarithm of (normalized) eigenvalues (λ) of the transfer matrix [25], is intuitively related to the spectrum of excitations made by all possible local operators with momentum quantum number k_x , $\lambda = |\lambda|e^{ik_x}$, at the minima of the spectrum [29].

The SCL can be generalized in two dimensions, however the momentum quantum number in the y direction

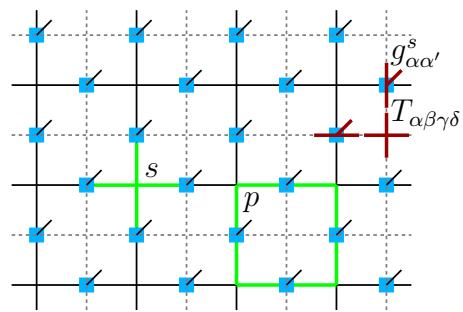


FIG. 2: A demonstration of the PEPS wavefunction of the toric code model in the σ^z basis. Green lines denote the star operator A_s and the plaquette operator B_p , and dark red lines denote the position of the 4-index T tensor and the 3-index g tensor, which are placed at the vertices and bonds of the dual lattice (denoted in dashed lines).

k_y is rigorously well defined as compared to the k_x estimated from the complex phases of the transfer matrix eigenvalues, as in the one-dimensional case mentioned above. Consider a cylindrical geometry (as in Fig. 1), we can define the SCL of the transfer matrix of a cylinder. If translation symmetry in the y direction is present, eigenvectors of the transfer matrix have well defined momentum quantum numbers k_y , and the minimum of the SCL is given by

$$\epsilon_{(k_x, k_y)} = -\ln(|\lambda_{(k_x, k_y)}^{\max}|/\lambda_0), \quad (2)$$

where $\lambda_{(k_x, k_y)}^{\max} = e^{ik_x} |\lambda_{(k_x, k_y)}^{\max}|$ is the leading eigenvalue of the transfer matrix with momentum k_y excluding ground states λ_0 s (the largest eigenvalue among all sectors); in general it is a complex number with a phase e^{ik_x} where k_x is its momentum in the x direction [29]. We conjecture that $\epsilon_{(k_x, k_y)}$ at a given (k_x, k_y) are analogous to the low-energy edge of the two-anyon scattering continuum described earlier. Thus, we propose that the minima of the SCL can be used to distinguish SET phases, by analogy with the dynamic structure factor. Next we will test this conjecture by examining the minima of the SCL of the transfer matrix.

Modified toric code model – To construct the simplest \mathbb{Z}_2 spin liquid which realizes all possible projective quantum numbers of the translation symmetry, we consider the toric code Hamiltonian on a square lattice

$$H = -K_e \sum_s A_s - K_m \sum_p B_p, \quad (3)$$

where $A_s = \prod_{l \in s} \sigma_l^x$ is defined on the vertex s and $B_p = \prod_{l \in p} \sigma_l^z$ is defined on the plaquette p , and the sum runs over all vertices and all plaquettes. This Hamiltonian has four degenerate ground states [30]. Depending on the signs of K_m and K_e , the quasi-particles e , m , if created, will move in a background of 0- or π -flux. That is, $\eta_e =$

$\text{sign}K_m$, $\eta_m = \text{sign}K_e$ in Eq. (1). The ground states on a torus can be simply represented by PEPSs of bond dimension $D = 2$. We now describe the PEPSs for all choices of $K_e = \pm 1$ and $K_m = \pm 1$.

The PEPSs are composed of 4-index tensors $T_{\alpha\beta\gamma\delta}$ at the vertices and 3-index tensors $g_{\alpha\alpha'}^s$ at the bonds of the direct (or dual) lattice, where s represents physical degrees of freedom and Greek letters represent virtual ones. Whether we take the direct or dual lattice depends on the choice of using a local σ^x or σ^z basis. Figure 2 represents a PEPS defined in the σ^z basis, where the tensor $T_{\alpha\beta\gamma\delta}$ is placed at the vertices of the dual lattice; this is the representation we choose throughout this paper unless specified otherwise. The virtual index runs from 0 to 1, where 0 means $|\uparrow\rangle$ and 1 means $|\downarrow\rangle$. The wave function has the form $|\psi\rangle = \text{Tr}\{T^{\otimes V} g^{\otimes B}\}$, where V means all vertices and B means all bonds, and the trace is taken over all common virtual degrees. The T -tensor is

$$T_{\alpha\beta\gamma\delta} = \begin{cases} 1, (0,0) & (\alpha + \beta + \gamma + \delta)\%2 = 0 \\ 0, (1,1) & (\alpha + \beta + \gamma + \delta)\%2 = 1 \end{cases}, \quad (4)$$

which, together with the condition that the only non-zero elements of the g -tensor are g_{ss}^s (see below), enforces the condition $B_p|\psi\rangle = +(-)|\psi\rangle$, corresponding to $K_m > 0$ ($K_m < 0$). The elements of the g -tensor are

$$g_{\alpha\alpha'}^s = \begin{cases} a, & \alpha = \alpha' = s = 0 \\ 1, & \alpha = \alpha' = s = 1 \\ 0, & \text{otherwise,} \end{cases} \quad (5)$$

where a is some number which can also depend on the position of the bond. We ask that the wave function satisfies $A_s|\psi\rangle = +(-)|\psi\rangle$ for $K_e > 0$ ($K_e < 0$); this is nothing but asking that the amplitudes for configurations related by flipping the four spins on the vertex s differ by $+(-)$. If $K_e > 0$ the solution is obvious: $a = 1$ on all bonds. However, if $K_e < 0$, it requires one and only one a on each plaquette of the dual lattice to be -1 , in which case one has to break the lattice translation symmetry in one direction in order to keep the bond dimension $D = 2$ (Supplemental Material [31]).

The excitations of the Hamiltonian Eq. (3) have no dynamics, which corresponds in the ground state $|\psi\rangle$ to the fact that all spin configurations satisfying Eq. (4-5) have equal weight in magnitude. To create some dynamics without increasing the bond dimension of the tensor, we put a local diagonal operator $\text{diag}(w, 1)$ on each physical spin with $0 \leq w \leq 1$, which corresponds to a ground state of the Hamiltonian [32, 33]

$$\begin{aligned} H' &= H + K_e \sum_s w^{-\sum_{l \in s} \sigma_l^z} \\ &\approx H + h \sum_l \sigma_l^z + \text{const.} \end{aligned} \quad (6)$$

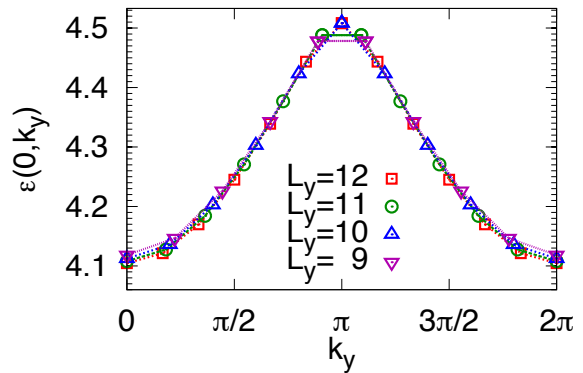


FIG. 3: The minima of SCL at momentum k_y for coupling $K_m > 0$ and $K_e > 0$ using PEPS at $w = 0.9$. Since all eigenvalues of the transfer matrix are real and positive, only $\epsilon_{(0,k_y)}$ is presented.

Here, the Zeeman field $h = -2K_e \log w$ is a good description of the perturbed state for $h \ll K_e$, or $w \approx 1$. Throughout this paper, we use $w = 0.9$, which corresponds to $h \ll |K_m|, |K_e|$ and is deep in the topologically ordered phase. For the phase diagram of the modified PEPS as a function of w in case of $K_m < 0$ and $K_e > 0$ (Supplemental Material [31]).

Numerical detection of the projective quantum number under translation symmetries – We take the PEPS wave functions described above and calculate the SCL of the transfer matrix [see Fig. 1(b)] for different signs of K_m and K_e . The transfer matrix of a cylinder with translation symmetry T_y can be block-diagonalized in momentum basis, which means each left and right eigenvector has a well defined momentum quantum number k_y . We start by explicitly writing the transfer matrix in real space into a block diagonal form in momentum space (Supplemental Material [31]). Once we have obtained the transfer matrix in momentum basis, we diagonalize each block with momentum $k_y = 2\pi m/L_y, m = 0, 1, \dots, L_y - 1$, find the minima of the normalized SCL $\epsilon_{(k_x, k_y)} = -\ln(|\lambda_{(k_x, k_y)}^{\max}|/\lambda_0)$, and plot $\epsilon_{(k_x, k_y)}$ as a function of k_y for $k_x = 0$ and π . Fig. 3 illustrates the minima of the SCL for $K_m > 0$ and $K_e > 0$, in which case, all eigenvalues of the transfer matrix are real and positive. The results for $K_m < 0, K_e > 0$ and L_y even are presented in Fig. 4: $\epsilon_{(0, k_y)}$ corresponds to the largest real and positive eigenvalue λ at each k_y excluding the two degenerate λ_0 s at $k_y = 0$, while $\epsilon_{(\pi, k_y)}$ corresponds to the smallest real and negative eigenvalue λ at each k_y . In the case of odd L_y for $K_m < 0$ and $K_e > 0$, matrices at each k_y further form into two non-commuting blocks, encoding the fact that applying the transfer matrix flips the eigenvalue of $\prod_l \sigma_l^z$, where the product is over a loop encircling the system in the y -direction. This corresponds to a breaking of translation symmetry (T_x) in a one-dimensional limit ($L_x \rightarrow \infty$ with L_y fixed). All eigenvalues of the transfer matrix come in \pm pairs, thus

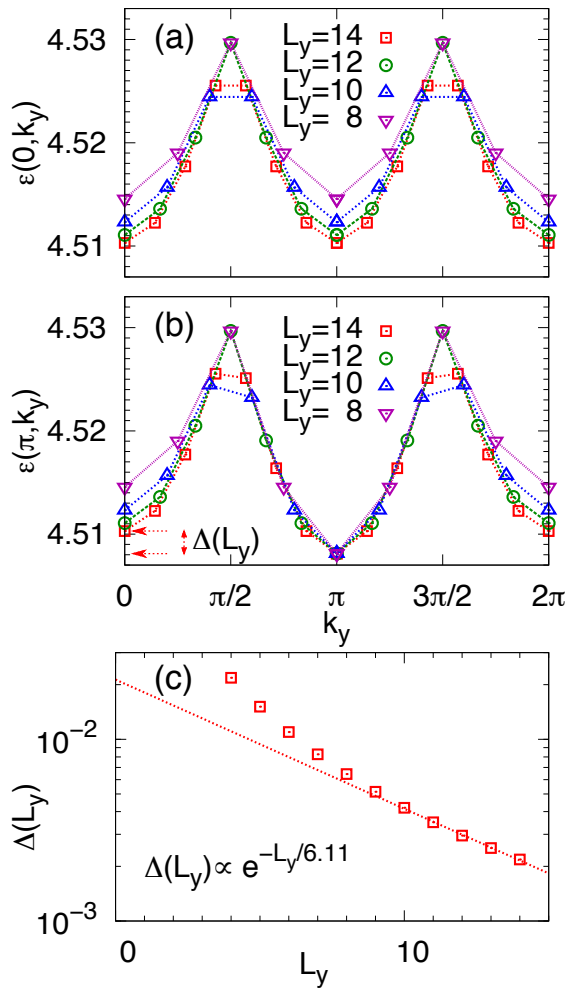


FIG. 4: The minima of SCL at momentum k_y for coupling $K_m < 0$ and $K_e > 0$ using PEPS at $w = 0.9$ for even L_y . (a) $\epsilon_{(0, k_y)}$ corresponds to the largest real and positive λ in sector k_y except λ_0 s. (b) $\epsilon_{(\pi, k_y)}$ corresponds to the smallest real and negative λ in sector k_y . (c) The splitting $\Delta(L_y) = \epsilon_{(\pi, 0)} - \epsilon_{(\pi, \pi)}$ as illustrated in (b) vanish exponentially as a function of length L_y .

$\epsilon_{(0/\pi, k_y)}$ are identical, as presented in Fig. 5. We find that the minima of the SCL are indeed doubly periodic when $K_m < 0$, but not when $K_m > 0$.

For the case of $K_e < 0$ and $K_m < 0$ ($K_m > 0$), the resulting $\epsilon_{(0, k_y)}$ are exactly the same as above, because the low-energy excitations are dictated by coupling K_m regardless of the sign of K_e . Note that when $K_e < 0$, $\epsilon_{(\pi, k_y)}$ is not accessible, because the transfer matrix at any L_y consists of adjacent two columns of the lattice, thus all eigenvalues are positive.

If we want the projective quantum number of m -particles, we can take a perturbed Hamiltonian as

$$H'' = -K_e \sum_s A_s - K_m \sum_p B_p + h' \sum_l \sigma_l^x \quad (7)$$

instead, and correspondingly choose a PEPS representa-

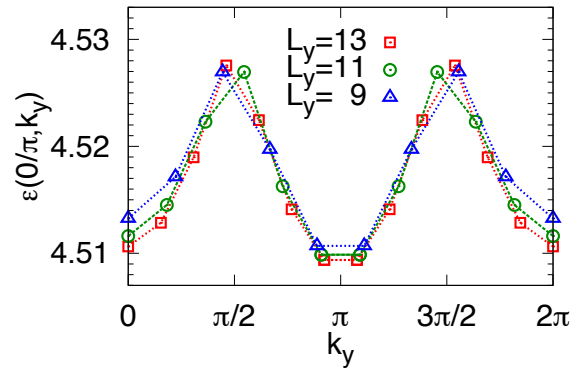


FIG. 5: The minima of SCL at momentum k_y for coupling $K_m < 0$ and $K_e > 0$ using PEPS at $w = 0.9$ for odd length L_y . Since eigenvalues including the largest come in \pm pairs, $\epsilon_{(0, k_y)}$ and $\epsilon_{(\pi, k_y)}$ are identical.

tion defined in the σ^x basis, where acting with a local operator $\text{diag}(w, 1)$ is equivalent to adding a perturbation $\delta H = h' \sum_l \sigma_l^x$. The low-energy excitations are two m -particles and the sign of K_e determines whether the m -particle hops in a background of 0- or π -flux on the dual lattice. Once the projective quantum numbers η_e and η_m are known, one completely determines SET class of the state if the symmetry group consists only of translation [2].

Conclusion – We have presented a numerical method to distinguish symmetry enriched topological (SET) phases with fractionalized translation symmetry. This method uses the spectrum of correlation lengths (SCL) of the transfer matrix on a cylinder to represent qualitatively the excitation spectrum of the system as a function of k_y for special $k_x = 0, \pi$, if the ground state wave function is available in terms of projected entangled pair state (PEPS). From the fact that the nontrivial fractional quantum numbers of quasi-particles under translation symmetries will be manifest as enhanced Brillouin zone periodicity in the dispersion relation, one can read out the projective quantum number of the low energy quasiparticles from the behavior of the minima of SCL. We bench-marked this method with the toric code model under perturbation. Modifying the sign of the coupling coefficients in front of operator A_s and B_p and the perturbation terms, we were able to generate topologically ordered ground states with preferred e -particle or m -particle low-energy excitations in a background of either 0 or π magnetic flux, which realizes all symmetry classes with this topological order and symmetry [2]. We expressed the ground states of the modified toric code Hamiltonians as bond-dimension $D = 2$ PEPSs and calculated the minima of the SCL of the transfer matrix on a cylinder, and the pattern of SCL revealed the fractional quantum numbers of the low energy quasiparticles under translation symmetries.

This method can be generalized to detect projective

quantum numbers of SET phases under a broader symmetry group including translations and other space group symmetries.

Acknowledgment – We would like to thank F. Verstraete and R. Mong for useful discussion. This work was supported by the Institute for Quantum Information and Matter, an NSF Physics Frontiers Center with support of the Gordon and Betty Moore Foundation through Grant GBMF1250, by the U.S. Department of Energy (DOE), Office of Science, Basic Energy Sciences (BES) under Award # DE-FG02-10ER46686 (M.H.), by Simons Foundation grant # 305008 (M.H. sabbatical support), and by the National Science Foundation through grant DMR-1206096 (O.M.).

-
- [1] L.-Y. Hung and X.-G. Wen, Quantized topological terms in weak-coupling gauge theories with a global symmetry and their connection to symmetry-enriched topological phases, *Phys. Rev. B* **87**, 165107 (2013).
- [2] A. M. Essin and M. Hermele, Classifying fractionalization: Symmetry classification of gapped Z_2 spin liquids in two dimensions, *Phys. Rev. B* **87**, 104406 (2013).
- [3] Y.-M. Lu and A. Vishwanath, Classification and Properties of Symmetry Enriched Topological Phases: A Chern-Simons approach with applications to Z_2 spin liquids, (2013), arXiv:1302.2634 (unpublished).
- [4] D. C. Tsui, H. L. Stormer and A. C. Gossard, Two-Dimensional Magnetotransport in the Extreme Quantum Limit, *Phys. Rev. Lett.* **48**, 1559 (1982).
- [5] R. B. Laughlin, Anomalous Quantum Hall Effect: An Incompressible Quantum Fluid with Fractionally Charged Excitations, *Phys. Rev. Lett.* **50**, 1395 (1983).
- [6] L. Balents, Spin liquids in frustrated magnets, *Nature* **464**, 199 (2010).
- [7] R. A. Jalabert and S. Sachdev, Spontaneous alignment of frustrated bonds in an anisotropic, three-dimensional Ising model, *Phys. Rev. B* **44**, 686 (1991).
- [8] A. Paramekanti and A. Vishwanath, Extending Luttingers theorem to Z_2 fractionalized phases of matter, *Phys. Rev. B* **70**, 245118 (2004).
- [9] S.-P. Kou and X.-G. Wen, Translation-symmetry-protected topological orders in quantum spin systems, *Phys. Rev. B* **80**, 224406 (2009).
- [10] C. Y. Huang, X. Chen and F. Pollmann, Detection of symmetry-enriched topological phases, *Phys. Rev. B* **90**, 045142 (2014).
- [11] F. Pollmann and A. M. Turner, Detection of symmetry-protected topological phases in one dimension, *Phys. Rev. B* **86**, 125441 (2012).
- [12] F. Verstraete and J. I. Cirac, Renormalization algorithms for Quantum Many Body Systems in two and higher dimensions, (2004), arXiv:cond-mat/0407066 (unpublished).
- [13] A. M. Essin and M. Hermele, Spectroscopic signatures of crystal momentum fractionalization, *Phys. Rev. B* **90**, 121102(R) (2014).
- [14] X.-G. Wen, Quantum orders and symmetric spin liquids, *Phys. Rev. B* **65**, 165113 (2002).
- [15] X.-G. Wen, Quantum order: a quantum entanglement of many particles, *Phys. Lett. A* **300**, 175 (2002).
- [16] F. Verstraete, V. Murg and J. I. Cirac, Matrix product states, projected entangled pair states, and variational renormalization group methods for quantum spin systems, *Adv. Phys.* **57**, 143 (2008).
- [17] F. Verstraete, M. M. Wolf, D. Perez-Garcia and J. I. Cirac, Criticality, the Area Law, and the Computational Power of Projected Entangled Pair States, *Phys. Rev. Lett.* **96**, 220601 (2006).
- [18] Z. C. Gu, M. Levin and X. G. Wen, Tensor-entanglement renormalization group approach as a unified method for symmetry breaking and topological phase transitions, *Phys. Rev. B* **78**, 205116 (2008).
- [19] Z. C. Gu, M. Levin, B. Swingle and X. G. Wen, Tensor-product representations for string-net condensed states, *Phys. Rev. B* **79**, 085118 (2009).
- [20] O. Buerschaper, M. Aguado and G. Vidal, Explicit tensor network representation for the ground states of string-net models, *Phys. Rev. B* **79**, 085119 (2009).
- [21] J. I. Cirac, D. Poilblanc, N. Schuch and F. Verstraete, Entanglement spectrum and boundary theories with projected entangled-pair states, *Phys. Rev. B* **83**, 245134 (2011).
- [22] D. Poilblanc, N. Schuch, D. Pérez-García and J. I. Cirac, Topological and Entanglement Properties of Resonating Valence Bond wavefunctions, *Phys. Rev. B* **86**, 014404 (2012).
- [23] N. Schuch, D. Poilblanc, J. I. Cirac and D. Pérez-García, Resonating valence bond states in the PEPS formalism, *Phys. Rev. B* **86**, 115108 (2012).
- [24] N. Schuch, I. Cirac and D. Pérez-García, PEPS as ground states: Degeneracy and topology, *Ann. Phys.* **325**, 2153 (2010).
- [25] S. Östlund and S. Rommer, Thermodynamic Limit of Density Matrix Renormalization, *Phys. Rev. Lett.* **75**, 3537 (1995).
- [26] X. Chen, Z.-C. Gu and X.-G. Wen, Classification of gapped symmetric phases in one-dimensional spin systems, *Phys. Rev. B* **83**, 035107 (2011).
- [27] N. Schuch, D. Pérez-García and I. Cirac, Classifying quantum phases using matrix product states and projected entangled pair states, *Phys. Rev. B* **84**, 165139 (2011).
- [28] F. Pollmann, A. M. Turner, E. Berg and M. Oshikawa, Entanglement spectrum of a topological phase in one dimension, *Phys. Rev. B* **81**, 064439 (2010).
- [29] V. Zauner, D. Draxler, L. Vanderstraeten, M. Degroote, J. Haegerman, M. M. Rams, V. Stojevic, N. Schuch and F. Verstraete, Transfer Matrices and Excitations with Matrix Product States, (2014), arXiv:1408.5140 (unpublished).
- [30] A. Kitaev, Fault-tolerant quantum computation by anyons, *Ann. Phys.* **303**, 2 (2003).
- [31] See Supplemental Material for PEPS construction of the ground state of toric code model with $K_e < 0$; the phase diagram of the PEPS by tuning parameter w for $K_m < 0$ and $K_e > 0$; and details of diagonalizing the transfer matrix of a cylinder in momentum basis.
- [32] C. Castelnovo and C. Chamon, Quantum topological phase transition at the microscopic level, *Phys. Rev. B* **77**, 054433 (2008).
- [33] N. Schuch, D. Poilblanc, J. I. Cirac and D. Pérez-García,

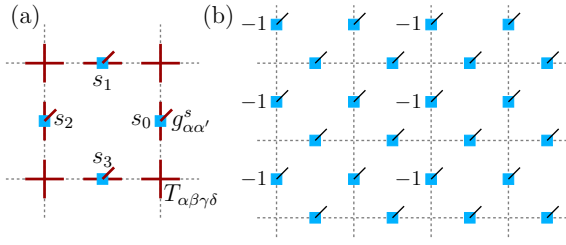


FIG. 6: (a) Demonstrate the vertices $T_{\alpha\beta\gamma\delta}$ and bonds $g_{\alpha\alpha'}^s$ affected by the operation of A_s on one plaquette of the dual lattice. (b) To meet the condition $A_s|\psi\rangle = -|\psi\rangle$, we choose $a = -1$ on the vertical bonds of every other column of the dual lattice (as marked by -1) and $a = 1$ for all other bonds (without mark).

Topological Order in the Projected Entangled-Pair States Formalism: Transfer Operator and Boundary Hamiltonians, Phys. Rev. Lett. **111**, 090501 (2013).

APPENDIX

PEPS for the ground state of toric code model with $K_e < 0$

In this section, we will discuss how to write a PEPS ground state for the toric code model with $K_e < 0$ while keeping the bond dimension $D = 2$.

We want to write the PEPS in the σ_z basis since our perturbation $h \sum_i \sigma_i^z$ is simple in this basis. The PEPS is composed of a 4-index tensor $T_{\alpha\beta\gamma\delta}$ of bond dimension $D = 2$

$$T_{\alpha\beta\gamma\delta} = \begin{cases} 1, (0,0) & (\alpha + \beta + \gamma + \delta) \% 2 = 0 \\ 0, (1,1) & (\alpha + \beta + \gamma + \delta) \% 2 = 1, \end{cases} \quad (8)$$

for $K_m > 0$ ($K_m < 0$), and a 3-index tensor $g_{\alpha\alpha'}^s$

$$g_{\alpha\alpha'}^s = \begin{cases} a, & \alpha = \alpha' = s = 0 \\ 1, & \alpha = \alpha' = s = 1 \\ 0, & \text{otherwise.} \end{cases} \quad (9)$$

Here a is a number and can be different at different positions in order to satisfy the following condition when $K_e < 0$

$$A_s|\psi\rangle = -|\psi\rangle. \quad (10)$$

The action of A_s is to flip four spins ϵ on the plaquette of the dual lattice as in Fig. 6(a). Assuming that each g -tensor at four positions s_0, s_1, s_2, s_3 in Fig. 6(a) shares the same constant a , then Eq. (10) means that $a^{4-2n} = -1$ for $n = 0, 1, \dots, 4$, where n is the number of down spins in that plaquette. However, there is no solution for the set of equations $a^0 = a^{\pm 2} = a^{\pm 4} = -1$. In conclusion,

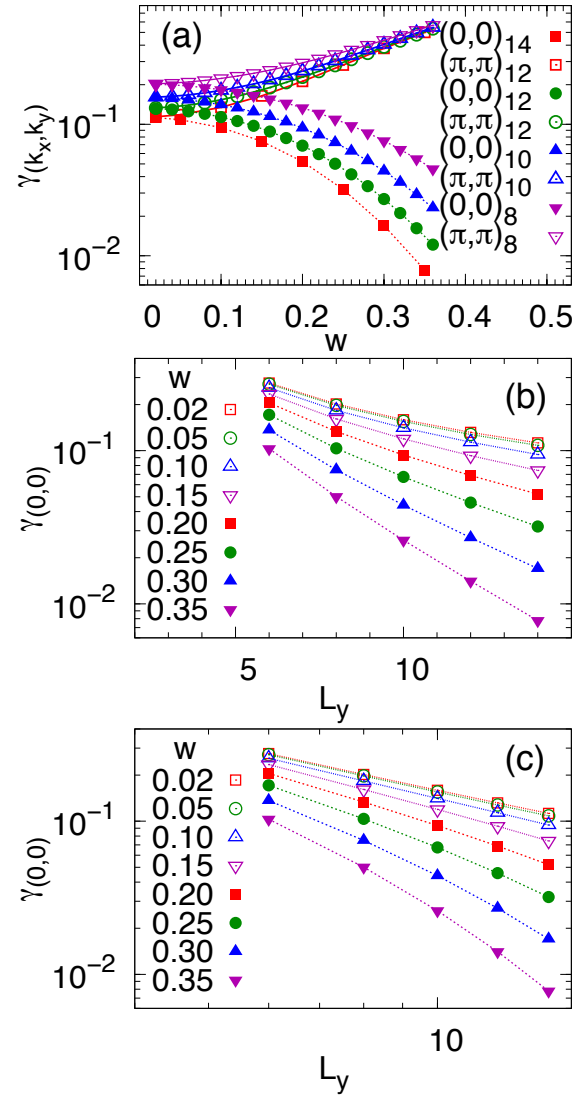


FIG. 7: (a) The ground state gap $\gamma_{(k_x, k_y)}$ for coupling $K_m < 0$ $K_e > 0$ as a function of w at special points $(0,0)$ and (π, π) for the cylinder perimeters $L_y = 8, 10, 12, 14$. For various fixed w , $\gamma_{(0,0)}$ is plotted against L_y in (b) a semi-log plot and (c) a log-log plot.

one has to break the translation symmetry and let a be different at different positions in one plaquette. We can choose a pattern as in Fig. 6(b) to satisfy Eq. (10) for every s . This choice maintains the translation invariance in the y direction but doubles the unit cell in the x direction; in such a case the transfer matrix consists of two adjacent columns instead of just one. We find that the minima of the SCL $\epsilon_{(0, k_y)}$ for $K_e < 0$ are identical with those for $K_e > 0$ if K_m is kept the same. This is expected since, in our system governed by Hamiltonian Eq. (6) in the main text, it is the e -particles that appear as low energy excitations and their dispersion is determined by the sign of K_m only (while the m -particles that are sensitive to the sign of K_e are still completely localized).

Phase diagram of the PEPS wavefunction by tuning parameter w for $K_m < 0$ and $K_e > 0$

This section studies the phase diagram of the PEPS wavefunction by tuning parameter w [in the local operator $\text{diag}(w, 1)$] from 1 to 0 for $K_m < 0$, $K_e > 0$. In one limit, when $w \approx 1$, the state is deep in the topologically ordered phase. In the opposite limit, $w \rightarrow 0$, all spins tend to point down, but the constraint Eq. 8 requires that each plaquette has an odd number of up spins. These conditions together lead to a state where all configurations with one spin up in each plaquette contribute equally.

When w is in between 0 and 1, one can imagine that the entropy contributed from the massive number of configurations that meet Eq. 8 is competing with the Zeeman energy, and a valence bond solid order could emerge. As one varies w from 1 to 0, the PEPS wavefunction could go through a phase transition from the topologically ordered phase to a valence bond solid phase. Inside the valence bond solid phase, translation symmetry is spontaneously broken in the thermodynamic limit, but at any finite size, the ground states are degenerate. We expect that two degenerate eigenvalues with ± 1 will appear as the leading eigenvalues of the transfer matrix; whereas in the topological phase, both leading eigenvalues are $+1$.

We now try to identify this phase transition using techniques discussed in the paper. We define $\gamma_{(k_x, k_y)}$, which roughly represents the gap to the ground state at momentum (k_x, k_y) , using eigenvalues of the transfer matrix:

$$\gamma_{(k_x, k_y)} = \begin{cases} -\ln(|\lambda_{(k_x, k_y)}^1|/\lambda_0), & k_x = k_y = 0 \\ -\ln(|\lambda_{(k_x, k_y)}^{\max}|/\lambda_0), & \text{otherwise} \end{cases}, \quad (11)$$

[in the sector $(0, 0)$ we take the subleading eigenvalue $\lambda_{(k_x, k_y)}^1$, otherwise the leading eigenvalue $\lambda_{(k_x, k_y)}^{\max}$]. $\gamma_{(k_x, k_y)}$ is different from $\epsilon_{(k_x, k_y)}$ defined earlier in that the splitting of λ_0 , doubly degenerate in the thermodynamic limit in the topological phase, is explicitly calibrated by $\gamma_{(0, 0)}$. We plot $\gamma_{(k_x, k_y)}$ at special points $(0, 0)$ and (π, π) as a function of w for cylinder perimeters $L_y = 8, 10, 12, 14$ in Fig. 7(a). Note that all other gaps lie well above these two within the plotted range. We do not see a crossing of $\gamma_{(0, 0)}$ and $\gamma_{(\pi, \pi)}$ as we vary w . Instead, we find that they approach each other, with $\gamma_{(\pi, \pi)}$ slightly larger than $\gamma_{(0, 0)}$ when w is close to 0. In order to examine finite size effects we plot $\gamma_{(0, 0)}$ as a function of L_y at various fixed w , in a semi-log plot [in Fig. 7(b)] and a log-log plot [in Fig. 7(c)]. The results are inconclusive; we cannot identify any critical point where a topological phase turns into a valence bond solid phase due to very large correlation length and insufficient system L_y size available.

Diagonalizing the transfer matrix of a cylinder in momentum basis

In the general case, the transfer matrix, denoted as \mathbb{E} , of a cylinder of circumference L_y can be thought of as a Hamiltonian for a system composed of local degrees of freedom with Hilbert space dimension D^2 (D is the bond dimension of PEPS) where each degree of freedom is composed of two virtual degrees of freedom. These local degrees of freedom are arranged in a ring with L_y “sites”. Note that the transfer matrix is generally not hermitian. The matrix elements of the transfer matrix in real space can be computed by specifying a basis vector $|a\rangle$ (which denotes compactly configuration of all L_y local degrees of freedom) and multiplying it by the transfer matrix

$$\mathbb{E}|a\rangle = \sum_b h_{ba}|b\rangle, \quad (12)$$

where $h_{ba} = \langle b|\mathbb{E}|a\rangle$ is the matrix element.

The transfer matrix commutes with translations T in the y direction and hence can be diagonalized simultaneously with T . The eigenvalues of T have the form e^{ik} where $k = 2\pi m/L_y$, $m = 0, 1, \dots, L_y - 1$. We construct the corresponding eigenspace V_k as follows.

First, we consider classes of real-space configurations that are related to each other by an action of T : $|a\rangle$ and $|a'\rangle$ belong to the same class if $|a'\rangle = T^\ell|a\rangle$ for some ℓ . It is easy to see that we can specify each class by one representative member $|a\rangle$, while all other members are given by $T^\ell|a\rangle$, $\ell = 0, 1, \dots, R_a - 1$, where R_a is the smallest number such that $T^{R_a}|a\rangle = |a\rangle$; the “periodicity” R_a must be less than or equal to L_y since $T^{L_y} = 1$. For a given momentum k , if kR_a is an integer multiple of 2π , then out of the states in this class we can construct a single normalized eigenstate of T with eigenvalue e^{ik} as follows:

$$|a_k\rangle = \frac{1}{\sqrt{N_a}} \sum_{r=0}^{L_y-1} e^{-ikr} T^r|a\rangle, \quad (13)$$

where N_a is the normalization constant

$$N_a = L_y^2/R_a. \quad (14)$$

On the other hand, if kR_a is not an integer multiple of 2π , we cannot construct such an eigenstate from the states in this class; thus this class of configurations is not compatible with the momentum k and is not included as a basis state for V_k . By going over all classes that are compatible with k , we construct a complete basis of V_k , which we call the momentum basis.

We calculate the transfer matrix elements in the basis

of V_k as follows

$$\begin{aligned} \mathbb{E}|a_k\rangle &= \frac{1}{\sqrt{N_a}} \sum_{r=0}^{L_y-1} e^{-ikr} T^r \mathbb{E}|a\rangle \\ &= \sum_{b'} h_{b'a} \frac{1}{\sqrt{N_a}} \sum_{r=0}^{L_y-1} e^{-ikr} T^r |b'\rangle, \end{aligned} \quad (15)$$

where $|b'\rangle$ runs over all real-space basis states. Each such $|b'\rangle$ belongs to some class whose representative we denote as $|b\rangle$, and hence there is $l_{b'}$ such that

$$|b'\rangle = T^{-l_{b'}} |b\rangle. \quad (16)$$

Substituting this in Eq. (15), we have

$$\mathbb{E}|a_k\rangle = \sum_{b'} h_{b'a} e^{-ikl_{b'}} \frac{\sqrt{N_b}}{\sqrt{N_a}} |b\rangle, \quad (17)$$

where the summation runs over all real-space basis states $|b'\rangle$ and not only the representative $|b\rangle$. Note that for each momentum-space basis state $|b_k\rangle$, the matrix element $\langle a_k | \mathbb{E} | b_k \rangle$ obtains contributions from all b' that belong to the class which corresponds to $|b_k\rangle$.

After finding the matrix elements $\langle b_k | \mathbb{E} | a_k \rangle$ in the basis in V_k , we can separately diagonalize the block diagonal transfer matrix for each momentum k and obtain the corresponding ϵ_{k_y} .

In the present case, the transfer matrix actually simplifies since the structure of the T and g tensors are such that the labels $\alpha\alpha'$ of the double tensor must coincide at each “site” in the transfer matrix; $\alpha_i = \alpha'_i$ and $\beta_i = \beta'_i$ ($i = 0, 1, \dots, L_y - 1$), thus the size of Hilbert space is reduced from D^{2L_y} to D^{L_y} .